

Accepted Manuscript

Biomechanics of the stick insect antenna: Damping properties and structural correlates of the cuticle

Jan-Henning Dirks, Volker Dürr

PII: S1751-6161(11)00183-4
DOI: [10.1016/j.jmbbm.2011.07.002](https://doi.org/10.1016/j.jmbbm.2011.07.002)
Reference: JMBBM 401

To appear in: *Journal of the Mechanical Behavior of Biomedical Materials*

Received date: 23 February 2011
Revised date: 28 June 2011
Accepted date: 1 July 2011

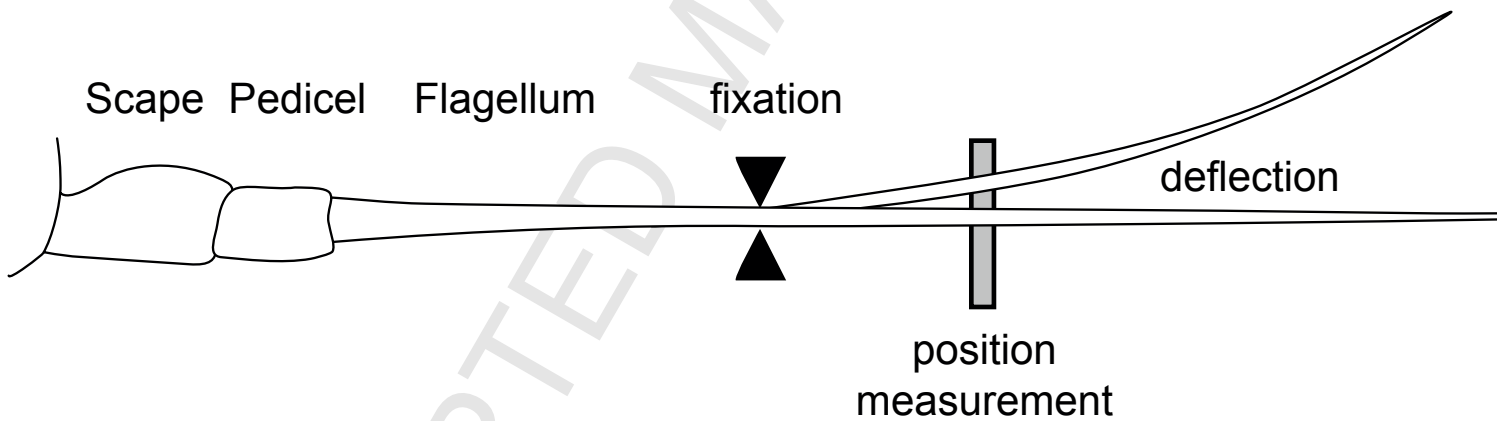


Please cite this article as: Dirks, J.-H., Dürr, V., Biomechanics of the stick insect antenna: Damping properties and structural correlates of the cuticle. *Journal of the Mechanical Behavior of Biomedical Materials* (2011), doi:10.1016/j.jmbbm.2011.07.002

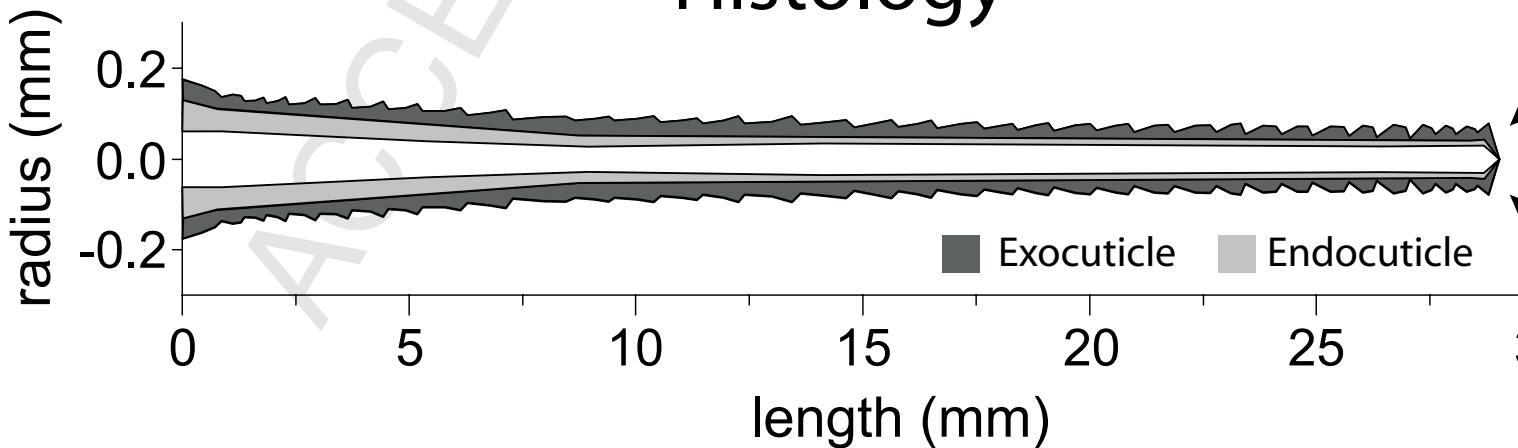
This is a PDF file of an unedited manuscript that has been accepted for publication. As a service to our customers we are providing this early version of the manuscript. The manuscript will undergo copyediting, typesetting, and review of the resulting proof before it is published in its final form. Please note that during the production process errors may be discovered which could affect the content, and all legal disclaimers that apply to the journal pertain.

Graphical Abstract

Passive deflection



Histology



Biomechanics of the stick insect antenna: Damping properties and structural correlates of the cuticle

Jan-Henning Dirks^{a,b,*}, Volker Dürr^{b,c}

^aPresent address: Dept. of Mechanical and Manufacturing Engineering,
Trinity College Dublin, Ireland

^bDept. of Biological Cybernetics, Bielefeld University, Germany

^cCognitive Interaction Technology - Center of Excellence, Bielefeld University, Germany

Abstract

The antenna of the Indian stick insect *Carausius morosus* is a highly specialized near-range sensory probe used to actively sample tactile cues about location, distance or shape of external objects in real time.

The length of the antenna's flagellum is 100 times the diameter at the base, making it a very delicate and slender structure. Like the rest of the insect body, it is covered by a protective exoskeletal cuticle, making it stiff enough to allow controlled, active, exploratory movements and hard enough to resist damage and wear. At the same time, it is highly flexible in response to contact forces, and returns rapidly to its straight posture without oscillations upon release of contact force. Which mechanical adaptations allow stick insects to unfold the remarkable combination of maintaining a sufficiently invariant shape between contacts and being sufficiently compliant during contact? What role does the cuticle play?

Our results show that, based on morphological differences, the flagellum can be divided into three zones, consisting of a tapered cone of stiff exocuticle lined by an inner wedge of compliant endocuticle. This inner wedge is thick at the antenna's base and thin at its distal half. The decay time constant after deflection, a measure that indicates strength of damping, is much longer at the base ($\tau > 25$ ms) than in the distal half ($\tau < 18$ ms) of the flagellum. Upon experimental desiccation, reducing mass and compliance of the endocuticle, the flagellum becomes under-damped. Analyzing the frequency components indicates that the flagellum can be abstracted with the model of a double pendulum with springs and dampers in both joints.

We conclude that in the stick-insect antenna the cuticle properties described are structural correlates of damping, allowing for a straight posture in the instant of a new contact event, combined with a maximum of flexibility.

Keywords:

biomechanics, insect cuticle, biomimetics, tactile exploration

1. Introduction

Many insects use antennae as tactile sensors to gain information about their environment. Antennae are leg-like appendages that have evolved to become dedicated sensory organs, combining various sensory modalities such as sound, gravi-, thermo- chemo- and in some cases probably even magnetoreception (Ferreira de Oliveira et al., 2010; Göpfert and Robert, 2001; Hansson, 1999; Sandeman, 1976; Tichy, 2007). They also mediate different mechanosensory cues provide tactile

information about the location and structure of objects and obstacles (Staudacher et al., 2005).

Specializing on active tactile exploration instead of visual senses can be advantageous for insects. First of all tactile senses are completely independent from ambient light, making them a useful sensory sensor organ for both, diurnal and nocturnal insects. Furthermore, the direct mechanical interaction of sensor organ and surface allows tactually guided course control (Camhi and Johnson, 1999; Cowan et al., 2006), adaptive control of climbing (Harley et al., 2009; Pelletier and Mcleod, 1994; Schütz and Dürr, in press) and tactile localisation and sampling of objects (Okada and Toh, 2006; Schütz and Dürr, in press; Zeil et al., 1985). This combination

*Corresponding author

Email address: jan-henning.dirks@tcd.ie (Jan-Henning Dirks)

of versatility with simplicity makes an insect antenna not only a fascinating biological sense organ; it makes it a model for artificial tactile systems that use only a single probe (Dürr et al., 2007; Hellbach et al., 2010) as an alternative to arrays of hair-like whiskers (Kim and Möller, 2007; Pearson et al., 2007; Solomon and Hartmann, 2006).

In this study we will focus on the biomechanical properties of the antenna of the Indian stick insect *Carausius morosus*. The stick insect is an important model organism in the control of adaptive locomotion. As flightless, nocturnal animals, stick insects strongly rely on tactile cues for obstacle detection and near-range orientation, which is why their long antennae are well-studied in the context of active tactile exploration (Dürr et al., 2001, 2003; Krause and Dürr, 2004; Schütz and Dürr, in press).

When actively exploring their environment, stick insects perform rhythmic antennal movements. This movement pattern is adapted to detect obstacles of critical height (Dürr et al., 2003), and antennal contact with obstacles can lead to rapid adaptation of ongoing leg movements (Schütz and Dürr, in press; Staudacher et al., 2005).

During this active tactile exploration, the antenna faces both non-contact and contact situations, imposing very different biomechanical constraints on both the execution of movement and the sensory processing of contact information. Since the cuticle is not only the exoskeleton of the antenna but also the supporting structure for a host of mechanosensory hairs (Monteforti et al., 2002; Slifer, 1966; Staudacher et al., 2005; Weide, 1960), at least four, partially conflicting, requirements can be formulated with regard to the function of an active tactile sensor: (1) First, being the protective surface structure, the cuticle has to be stable and hard enough to withstand damage and wear; (2) Second, both the control of movement and the sensory localisation of contact events would be simpler for a stiff and straight beam than for a compliant, hose-like structure. This is because high stiffness leads to little change in shape and, consequently, little need for proprioceptive monitoring of shape changes. Indeed, previous studies have shown that the shape of the flagellum of *C. morosus* and other insects changes very little at all during contact-free, exploratory movements (Dürr et al., 2001) and during flight (Heinzel and Gewecke, 1987). (3) Third, high stiffness would imply that physical contact of a long and thin flagellum with an object gives rise to large torques which could break and destroy the sensory organ. Therefore, compliance is important, too. Indeed, a number of studies have shown that arthropod antennae

can undergo large deformations during obstacle contact (Camhi and Johnson, 1999; Lee et al., 2008; Sandeman, 1989 and see also suppl. video material of Schütz and Dürr, in press). (4) Finally, stiff structures must be damped if high-frequency oscillations (and associated sensory noise) are to be avoided (Loudon, 2005; Staudacher et al., 2005), and compliant structures must be damped if post-contact return to the original shape is to be as fast as possible. The latter consideration indicates that damping might be the critical parameter to minimize the trade-off between little change in shape (high stiffness) and flexibility (high compliance).

Here we ask how insect antennae mechanically combine these requirements of structural deformation and mechanical controllability and stability. What role does the biomechanics of the antenna's structure and, in particular, its material play?

1.1. General morphology of insect antennae

In *Carausius morosus*, as in most stick insect species, the antenna is long, thin, and not serrated, typical for antennae of the filiform type (Weber, 1968). As in all ectognathous insects, the antenna can be divided into three functional morphological units: scapus, pedicellus and flagellum (Imms, 1939). In *C. morosus* the scapus is typically 0.8 mm in diameter, 1.7 mm long and connected to the caput with a dycondylar joint (Dürr et al., 2001). Two different groups of muscles control the movement of the scapus: whilst the two levator muscles move the scapus in dorsal and ventral direction, the contractions of the depressor muscle result in movements in medial and lateral direction (Dürr et al., 2001).

The pedicellus is typically 0.8 mm long with a basal diameter of 0.5 mm. It is moved by two antagonistic muscles located within the scapus (Dürr et al., 2001). The lateral scapo-pedicellar muscle moves the pedicellus in the ventro-lateral axis, whilst dorso-medial movements are caused by contractions of the medial scapo-pedicellar muscle. The movement-axes of caput-scapus and scapus-pedicellus are slanted and non-orthogonal, which has been interpreted as an adaptation to increased vertical and horizontal positioning resolution (Krause and Dürr, 2004; Mujagic et al., 2007).

The flagellum of *C. morosus* has a typical length of 35 mm and cannot be moved actively (Dürr et al., 2001; Imms, 1939). It is subdivided by a number of radial furrows that separate more or less convex annuli ("ringlets", 40-46 annuli according to Monteforti et al., 2002). These annuli are not true segments and do not have any structural correlate below the cuticle (see suppl. figure 6). Although previous studies have studied and described the general morphology and function

of other insect antennae, very little is known about the detailed histology of the flagellum's cuticle.

1.2. Histology of the flagellum

Looking at the relative proportion of cuticular tissue, the flagellum can be simplified as a composite structure with two distinct, mechanically relevant layers: the outer exocuticle and the inner endocuticle. The outer exocuticle layer provides structural support and important protection against external factors, such as for example parasites or predators. In general, the stiff exocuticle of locusts ($E=9.6$ GPa) shows only very poor damping properties whilst the much softer, 'rubber-like' endocuticle ($E=2$ MPa) shows strong damping properties for oscillations above 100 Hz (Jensen and Weisfogh, 1962).

Previous studies have also shown structural correlates between composite materials and physical properties in various biological systems, including bacteria, molluscs, vertebrates and insects (Hepburn and Chandler, 1976; Lin et al., 2009; Mayer and Sarikaya, 2002; Sun et al., 2008; Williams and Kramer, 2010). It thus seems likely that the distinct physical properties within the flagellum's cuticle might correlate with its unique physical properties, combining stiffness with flexibility and controllability. The stiff exocuticle might provide the required stiffness to move and control the flagellum during active exploration whilst the soft endocuticle might act as a biological "damping system", reducing unwanted oscillations of the flagellum.

The present study combines histological, morphological and biomechanical experimental approaches to characterize the mechanical properties of the flagellum of the *Carausius morosus* antenna. In particular, we looked for correlations between histology and the biomechanical characteristics. We were able to show that the specialized layering of the flagellar exo- and endocuticle, and in particular the water content, significantly affects its biomechanical properties. As the compliance of endocuticle is thought to be due to its high water content (Mueller et al., 2008; Vincent and Wegst, 2004), this indicates a critical role of the endocuticle.

2. Material and Methods

2.1. Morphological measurements and cuticle layering

Adult, female stick insects of the species *Carausius morosus* (Sinéty 1901) were taken from laboratory colonies at the University of Bielefeld, Germany. For morphological measurements, antennae were cut off and studied using standard light microscopy. A series of

digital photographs was taken to document the number, size and shape of all annuli along the flagellum. All measurements were made using a custom written program. The spatial resolution depended on magnification and ranged between 0.6 and 1.6 μm per pixel.

To measure the thickness of cuticle layers the antennae were cut off and divided into three parts, fixed in Bouin's solution for 24 h, embedded in paraffin by standard routines, and cut on a microtome into stacks of transverse sections of 10 μm thickness. Sections were then mounted to slides, stained with Heidenhain's Azan (Romeis, 1989) and immersed in epoxy resin. The Azan staining allows clear distinction of sclerotised exocuticle (orange staining) from unsclerotised endocuticle (blue), nerve tissue (grey) and cell bodies of hypodermis or sensory cells (both red, see figure 3 and suppl. figure 6).

From each antenna, four regions were sectioned into stacks, and five sections were selected from each stack. The four sectioned regions were the distal pedicel and three parts of the flagellum, i.e. base, middle and tip. In the basal part of the flagellum, sections were taken from the proximal region of the stack, in the middle part sections were taken from the central region of the stack, and in the distal part sections were taken from the distal region of the stack. Within each section, the cuticle layer thickness was measured at three points, approximately spaced by 120 degrees. Therefore, our choice of sampling includes both radial and longitudinal variability within a given region of the pedicel or flagellum. Spatial resolution was 0.54 μm per pixel in proximal sections (pedicel and base) and 0.21 μm per pixel in distal sections (middle and tip).

2.2. Damping properties

Damping properties of the flagellum were determined optically and contact-free by measuring the passive return time course of the flagellum after a step deflection (see figure 1). Insects were mounted *in toto* to a platform. The head as well as the first two segments of the antennae (scape and proximal part of the pedicel) were immobilized using dental cement (Protemp, ESPE). The platform could be moved by a micromanipulator next to a light-microscope and adjusted such that flagellum was held just above a one-dimensional, high-speed, position-sensitive photodiode, PSD (Hamamatsu S3931; active area: 6x1 mm; rise time: 1.5 μs ; maximum spatial resolution: 0.2 μm). The white light of the microscope lens was then focused on the surface of the PSD, so that the flagellum casted a sharp shadow onto the sensor area of the PSD. The voltage difference ΔU across the PSD was proportional to the shadow

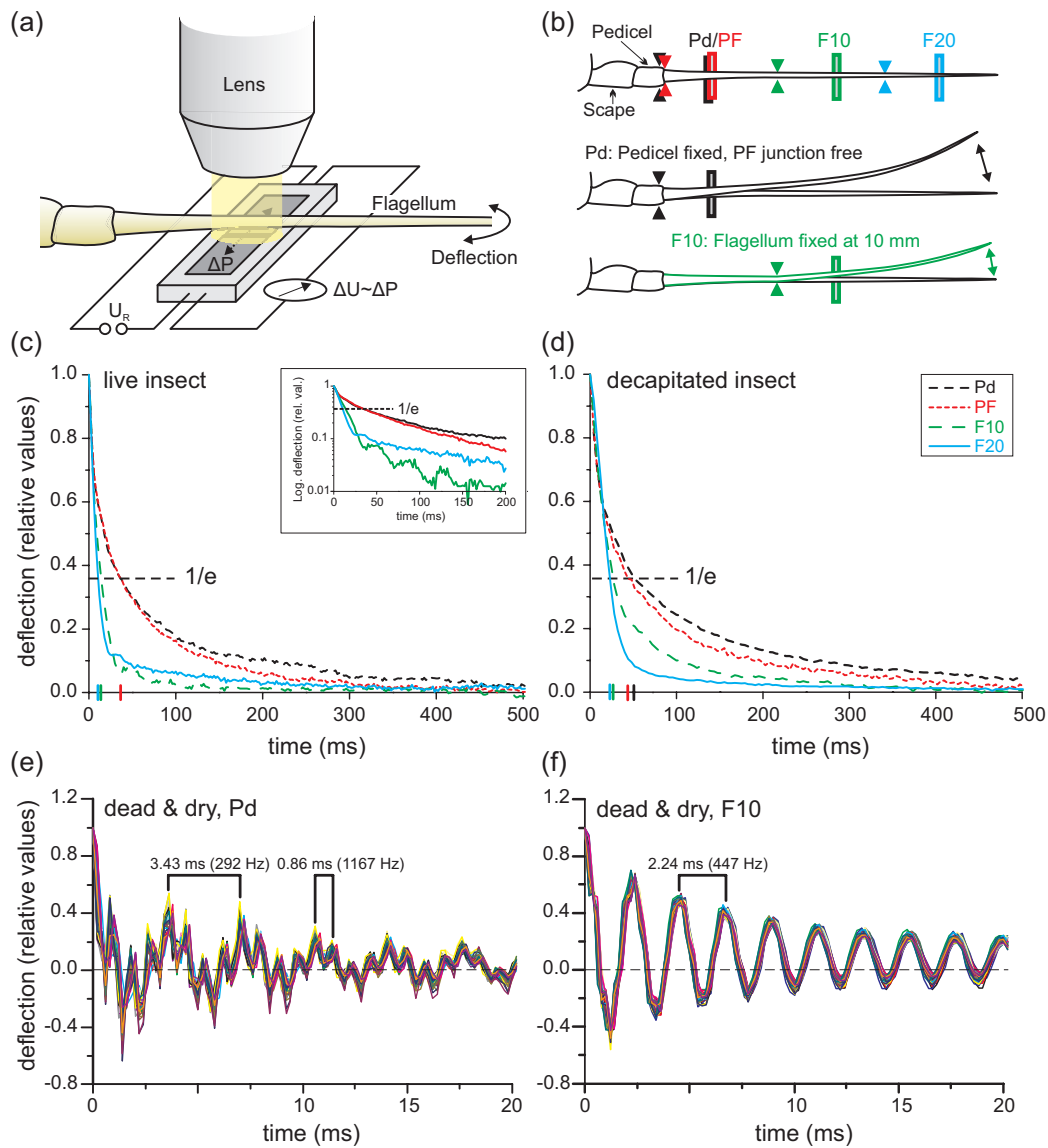


Figure 1: (a) Over-damped return from mechanical deflection was measured using a position-sensitive photodiode (PSD). For details see text. (b) Schematic illustration of the fixation and measurement sites along the antenna (triangles indicate fixation site, rectangles indicate sensor position): In the reference condition, the antenna was fixed at the pedicel, leaving the pedicel-flagellum junction free (Pd, black). Additional fixation of the PF junction (red); and additional fixation at 10 mm (F10, green) and 20 mm (F20, blue) along the flagellum. (c) and (d) Return time courses from deflection in a live and a decapitated insect. Time courses were faster than expected for a single exponential (see semi-logarithmic plot in insert). Proximal fixation (conditions Pd and PF) resulted in stronger damping than distal conditions F10 and F20. (e) and (f) Drying of the antenna resulted in sustained oscillations with strong overshoot for all fixation conditions. Superimposed time courses from 39 trials of the same preparation illustrate the stereotypic nature of the return movements.

displacement of the antennae ΔP (see figure 1 a). A custom-built amplifier transformed the voltage difference into a contrast measure that was robust against changes in light intensity. The output signal of this amplifier was sampled by an AD converter system (CED 1401 power, controlled by Spike2 software, Cambridge Electronics Design) at 5 kHz sampling rate. Return time measurements were acquired for four different fixation sites (see figure 1 b):

1. the distal pedicel (condition Pd), leaving the entire flagellum unrestrained, including the pedicellus-flagellum junction.
2. fixing the pedicellus-flagellum junction (condition PF), leaving the flagellum unrestrained, but not its connection to the pedicel.
3. fixing the proximal 10 mm of the flagellum from the base (condition F10), leaving the distal two thirds of the flagellum unrestrained
4. fixing at the middle of the flagellum, 20 mm from the base (condition F20), leaving only the distal third of the flagellum unrestrained

In each condition, the PSD was placed 5 mm distal to the fixation site, such that displacements of the flagellum always corresponded to the same angle of deflection (see figure 1).

After restraining the flagellum at one of the four fixation sites, it was deflected manually by means of a minuten pin that was held by a lever arm (similar to a record-player arm). This lever arm could be rotated in the horizontal plane, causing the pin to push against the flagellum and deflect it. By inclining the arm by a few degrees the flagellum was abruptly released from the pin and passively swung back to the initial position. The contact point of pin and flagellum was always 10 mm distal from the fixation site. Other contact points were tested as well but will not be presented here, as the results were equivalent. The contact force caused the flagellum to bend in the region between the fixation and the pin. After a brief holding time, the flagellum was released and snapped back passively to its starting position. The time course of this return was recorded by the PSD. Measurements were repeated at least 5 times per fixation site and contact site.

In order to account for possible directional anisotropies in the biomechanics of the flagellum, animals were first mounted in a dorsal-side-up orientation and then later in a pleural-side-up orientation. In the first set of measurements, the antenna was deflected medially and laterally. In the second set of measurements, the antenna was deflected dorsally and ventrally. To account for possible effects of order, the

dorsal-ventral and medial-lateral pairs were randomly varied for each insect.

For data analysis, time courses of 1 s duration (equiv. to 5000 values) were manually extracted, beginning with the distinct sharp onset of the position change of the flagellum. Data were then filtered, using a binomially weighted sliding window of 2.2 ms width. The baseline was determined as the average value within the last 40 ms of the time course. This was subtracted from all values. For the analysis of decay constants, time courses were normalized with respect to their maximum deflection amplitude. Decay time constants were determined in two ways. Assuming a first-order exponential decay, we determined the time constant τ_e , the time at which the flagellum had returned to 36.8 % of its maximum deflection ($1/e = 0.368$). A second measure of the decay time constant was calculated from the slope m of the log-transformed time course within the first 10 ms of the decay: $\tau_{10} = -1/m$.

Qualitatively, both values of τ yielded equivalent results and the choice of method had no effect on any claims made by this paper. Nevertheless, as the time courses deviated from a true first-order exponential (see figure 1 c and corresponding text), we focus on the second calculation method in this paper.

To determine the effect of haemolymph pressure and of water content in the endocuticle, stick insects were decapitated by transection of the head at the level just behind the eyes. The transection cut was immediately sealed with dental cement to prevent the antenna from drying out during the experiments. Following reference measurements on the decapitated animals, the dental cement was carefully removed and head and antenna were desiccated in a drying chamber for 36 h at 50 °C or for 48 h at 30 °C. To quantify the loss of water, the antennal segments were weighted directly before and after the desiccating process (Sartorius scale, 1801, 0.01 mg). Neither the temperature nor the time of desiccation affected any of the results presented in this study. Measurements on decapitated and/or dried animals followed exactly the same protocol as described for live animals. For desiccated animals, measurements for fixation site F20 turned out to be impossible because the flagellum always broke during the first return.

2.3. Statistics

Data was tested for homogeneity of variances and normal distribution. To test for differences between groups we performed analyses of variance (ANOVA) and, where specified, Tamhane posthoc tests. If not stated otherwise, summarized values represent means with standard deviation.

3. Results and Discussion

3.1. Summary

At first we show that the flagellum of the stick-insect antenna can be divided into three morphological zones with distinct characteristics of the annuli. In a next step, we studied the histology of cuticle layering in these three zones. We found that the ratio of soft endocuticle to stiff exocuticle differed between proximal and distal parts of the flagellum. If damping was related to endocuticle, this would suggest that damping should be different along the antenna. Damping experiments with living, decapitated and desiccated insects validated this hypothesis and showed that the endocuticle core seems largely responsible for the damping properties of the flagellum.

3.2. General morphology of the flagellum

In the stick insect flagellum, the shape, length and mass of each annulus, but also the number of sensory hairs carried by it, differ considerably (see figure 2 and supplemental figure 5). The number of annuli was very variable and ranged from 34 to 43 (median: 36), which was slightly less than the 40-46 reported by (Monteforti et al., 2002). In two animals, annuli of both antennae were analyzed. In both of these animals, annulus number and length distribution was not equal on both sides. The average measures in figure 2 show a hypothetical mean flagellum with 36 annuli (first 18 annuli for proximal, last 18 annuli for distal). The length of the flagellum ranged from 28.7 to 30.1 mm (median: 29.5 mm). Together with the scape (1.7 mm) and pedicel (0.8 mm), this results in an average length of 32 mm. This length corresponds very well to the length of an out-stretched front leg, such that the frontal action range of the antenna closely overlaps with that of the front leg.

Annulus diameter is largest at the base and decreases towards the tip, with strongest tapering occurring in the first quarter of the flagellum (see figure 2 a). Over the first ten annuli, the base diameter drops by 45.3 % from $351 \pm 39 \mu\text{m}$ to $192 \pm 23 \mu\text{m}$. The gradual change in annulus shape can be seen by comparison of the three values per annulus. In the proximal and middle regions of the flagellum, annuli are characterized by a distal widening, i.e., the largest diameter is found near the distal end of each annulus. An exception to this rule is the very first annulus, which has the shape of a tapered cone. In the distal quarter of the flagellum, annuli are characterized by a rounded, bead-like shape. Here, the largest diameter is in the middle.

Annulus length also changes along the flagellum (see figure 2 b). Following a first, rather long annulus, length suddenly decreases at annulus two and then steadily increases over the following ten annuli. After that, the middle of the flagellum is characterized by very long annuli, interspersed by occasional very short ones. Typically, both the shortest and longest annuli were found in this part of the flagellum (range: 0.21 to 1.96 mm). As a result, both the range and the variance of annulus length are very large (median range: 1.18 mm; max. standard deviation: 0.4 mm). In the distal quarter, annulus length decreases towards the tip.

All annuli carry different types of sensory hairs that differ in size, shape and sensory modality (Monteforti et al., 2002; Sliifer, 1966; Weide, 1960). Together, these sensilla cause a drastic increase of the surface area of the antenna and, as a result, most likely increase the aerodynamic drag compared to a hairless antenna. The density of sensilla per unit surface area can serve as an indicator whether or not sensilla-induced drag forces change along the flagellum. We counted only the lateral hairs that lay within the focal plane of the light microscope, assuming that hair density is equal around the circumference of each annulus. As an estimate of annulus surface area, we chose the surface of a cylinder. The cylinder dimensions were set to the length and central diameter of the annulus. Sensilla density increases from the base towards the tip (see figure 2 c). Judged from histological sections (see figure 2 a) and scanning electron micrographs (not shown), the packing of sensory hairs on the most distal annulus is so high, that it is likely to represent an upper limit.

On the grounds of the external features described, the flagellum can be morphologically subdivided into three zones (dashed lines in figure 1, figure 3 c). Zone I, (base) comprises the proximal quarter, where the annulus diameter decreased and length first decreased abruptly only to increase until annulus 10. The sensilla density was low. In zone II (mid), beginning at annulus 11, the mean annulus length and distal diameter remained almost constant, but annulus length was very variable. Sensilla density increased by more than 190 %. Annulus 11 had a distinctly smaller diameter and usually was considerably longer than annulus 10, which carries a dorsal thermosensory organ with the shape of a distinct swelling (Altner et al., 1978; Cappe de Baillon, 1936). In zone III at the tip of the flagellum the annulus shape was oval, being widest in the middle. The length of the annuli decreased and sensilla density was almost equal.

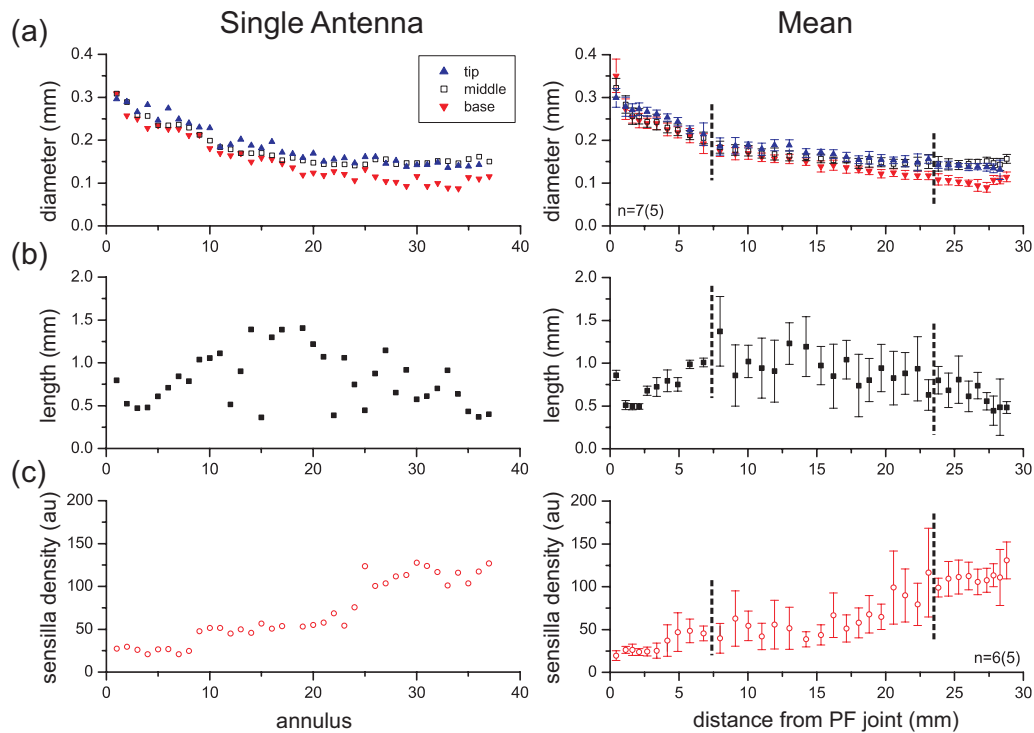


Figure 2: Left: data of a single antennal flagellum for each annulus with increasing number from proximal to distal. Right: Mean and standard deviation of seven antennae along the flagellum. (a) Annulus diameter measured at the proximal base, in the middle and at about 90 % of annulus length. Mean values (right panel) show that all three measures decrease towards the tip. In proximal annuli, 90 % length is equivalent to the widest region. The different gradual change of the three measures reflects a gradual change in annulus shape. (b) Annulus length. Distally from annulus 1 and 2, the length increases within region I, is very variable in middle annuli (region II), and decreases towards the tip (region III). (c) Relative density of sensilla per unit surface, expressed in arbitrary units (au, see text). Sensilla density increases towards the tip.

3.3. Ratio of endo- and exocuticle along the antenna

Hepburn and Chandler (1976) state that the sclerotised exocuticle dominates the stress-strain relationship of cuticle (until fracture), whereas the non-sclerotised endocuticle determines the damping properties. Based on this conclusion, we focused on the layering of exo- and endocuticle of the antenna. Figure 3 shows histological cross sections taken through the pedicel and the three zones of the flagellum, as described above. Cuticle layering differed strongly between proximal and distal parts of the flagellum. In the pedicel and zone I of the flagellum (base), the endocuticle layer (blue) was of similar thickness as the exocuticle layer (orange). In zones II and III (mid and tip), the exocuticle was noticeably thicker than the endocuticle (see figure 3 b and

suppl. figure 6).

At the flagellum base (zone I), the endocuticle was of similar average thickness as in the pedicel (pedicel: $17.0 \pm 4.6 \mu\text{m}$; zone I: $15.5 \pm 1.4 \mu\text{m}$, $N=15$ measurements from 3-5 insects), but decreases down to $4.2 \pm 1.4 \mu\text{m}$ (27 %) in the middle of the flagellum (zone II) and to $1.6 \pm 0.9 \mu\text{m}$ (11 %) at the tip (zone III). The exocuticle of the pedicel was, on average, slightly thinner than the endocuticle. Exocuticle thickness increased at the basal flagellum (pedicel: $12.1 \pm 1.4 \mu\text{m}$; zone I: $18.4 \pm 1.0 \mu\text{m}$), maintained about the same thickness throughout the middle of the flagellum (zone II: $17.2 \pm 1.2 \mu\text{m}$, 93 % of zone I) and decreased to $8.3 \pm 2.2 \mu\text{m}$ (45 %) at the tip. As a result, the average thickness ratio of the two cuticle layers decreased

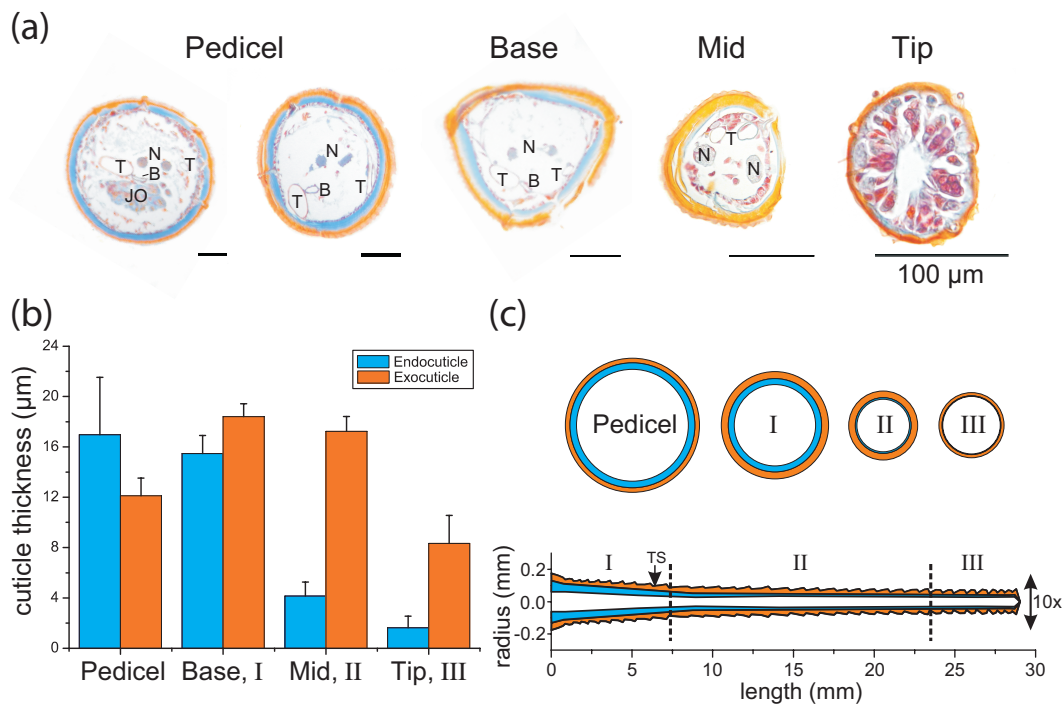


Figure 3: (a) Azan-stained transverse sections of the antenna, showing exocuticle (orange) and endocuticle (blue). Sections were taken through the central pedicel, distal pedicel, zone I (base), zone II (mid) and zone III (tip) of the flagellum. Labels indicate two branches of main antennal nerve (N), the blood vessel (B), Johnston's organ (JO) and tracheae (T); scale bars are 100 μm. (b) Thickness of exocuticle (orange) and endocuticle (blue) at different positions along the antennae. Thickness of the endocuticle decreases from the pedicel toward the tip of the flagellum whilst exocuticle is thickest in basal and middle annuli of the flagellum. Three measurements were taken from each one of five cross sections per preparation. (zone III: N=5 animals, n=75 measures; else: N=3, n=45, mean±SD). (c) Top: Schematic average cross sections of the *C. morosus* flagellum, drawn to scale. Bottom: Schematic longitudinal section, based on data from figure 1. For clarity, the figure is expanded radially by a factor of 10 and not drawn to scale. The diameter decreases towards the tip, the radial furrows between the annuli become deeper toward the tip. The three flagellum zones are labelled I to III (for details see text).

monotonically from pedicel to zone III (pedicel: 1.40; base: 0.84; mid: 0.24; tip: 0.20).

As yet, stiffness and damping of the antenna do not only depend on overall cuticle layer thickness but also on the ratio of the cross-sectional areas covered by the two distinct layers (see table 1). The fraction of cross section area covered by sclerotised cuticle was largest in the middle of the flagellum, where it exceeds 46%. It was only little less in zone I (43.6%) but considerably lower at the pedicel and at the narrow tip. This situation was contrasted by the strongly different fractions of cross-sectional area covered by soft endocuticle. The latter exceeded 18% at the basal zone I, but remained less than 8% in the mid zone II. The ratios of exo- and endocuticle layers are illustrated by the schematics in

figure 3 d. Note that basal and medial annuli of flagellum zones I and II are not linked by a soft endocuticle, as it occurs in the arthrodial membranes of true joints. Rather, the stiff exocuticle forms a thick connection. In the most distal annuli of zone III, the annulus junction has only a very thin exocuticle layer. Here, the compliant endocuticle dominates the junction (see figure 6). As a consequence, the cuticle layering “within annuli”, as reported above, will strongly affect bending and damping at the base and in zones I and II of the flagellum.

In summary, the histological results on cuticle layering strongly suggest that the biomechanical properties (stiffness and damping) of the flagellum should differ between proximal and distal parts of the flagellum. En-

docuticle, with a much higher water content than exocuticle, is known for its biomechanical damping properties (Jensen and Weisfogh, 1962; Vincent and Wegst, 2004). Hence, the thick endocuticle layer at the base of the flagellum and its large fraction of the cuticle's overall cross-sectional area should result in strong damping of movements imposed on the proximal part of the flagellum. Moreover, a thinner endocuticle in distal parts of the flagellum should result in weaker damping.

3.4. Damping properties of the flagellum

We tested the latter hypothesis by measuring the return time course of the flagellum after bending it at different locations along the flagellum (see figure 1 a). This was accomplished by fixing the flagellum at one of four alternative points (see figure 1 b). The choice of fixation sites allowed us to address the following three objectives:

1. What is the damping mode of the antenna flagellum? (under-damped, critically damped, or over-damped)
2. Does the damping coefficient decrease from the base towards the tip?
3. Does the pedicellus-flagellum junction contribute to damping?

To address the first objective, we tested whether or not the return time courses exhibited an overshoot and quantified this by measuring the decay time constant. To answer the second question we fixed the flagellum either at the PF-junction (condition PF) or 10 mm or 20 mm distally from the PF-junction (conditions F10 and F20), i.e. at the beginning or end of zone II (compare with figure 2). For the third objectives, we compared the return time course of the flagellum when the antenna was fixed at the distal pedicel (condition Pd) only with the PF condition additionally fixed.

Table 1: Cross-sectional areas of the pedicel and the three flagellum zones (based on data of figure 3). The cross section of the antennae was assumed to be a perfect circle. This simple assumption holds well for the pedicel and the tip, but deviates in the middle of the flagellum, where the cross section can be slightly triangular.

	cross section (mm ²)	% of cross-sectional area	
		Exocuticle	Endocuticle
Pedicel	0.096	13.4	17.1
Base	0.058	25.2	18.4
Middle	0.020	38.3	7.9
Tip	0.018	21.0	3.8

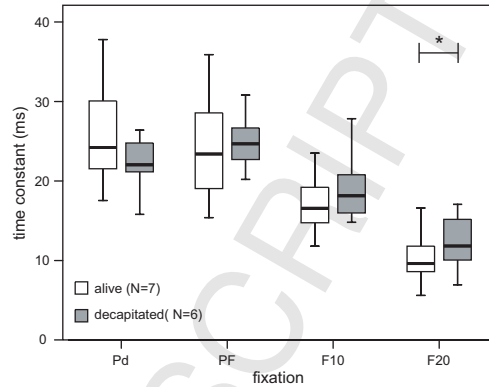


Figure 4: Time constants (τ_{10}) of decay time courses from antennae of alive/intact and dead/decapitated stick insect antennae. Measurements were repeated for four different fixation sites. Decapitation had very little effect on the time constant. The only significant effect was found at the most distal fixation site, F20. For details see text.

Typical return time courses of a live insect are shown in figure 1 c. The returning movement of the flagellum was over-damped in all conditions tested. This corroborates observations on the antennae of *Locusta migratoria* (Heinzel and Gewecke, 1987).

In all four conditions, the time course resembled a first-order exponential decay for the initial 20 to 30 ms, as can be seen by the straight initial decay in the logarithmic plot of the insert to figure 1 c. After this initial period, the decay was slower than what would be expected for a simple first-order exponential with a constant decay factor. In the fastest decays (as found for fixation at F10 or F20) oscillations were seen regularly, though not in all trials (F10: 21.7 % of trials, N= 420; F20: 61.0 % of trials, N= 344).

Oscillations of the flagellum were very rare for both proximal fixation sites (Pd: 3.2 %, N= 402; PF: 7.7 %, N= 416). The occasional presence of small oscillations suggests that the mechanical system is very close to critical damping, particularly in distal zones.

Generally, the time constant τ_{10} was shorter than τ_e , indicating that the initial decay was faster than expected from a single exponential decay (see figure 1 c). Measured values of τ_{10} are summarized in figure 4 and were 27.0 ± 9 ms and 25.2 ± 9 ms for conditions Pd and PF, respectively (Pd: N= 588; PF: N= 590). For distal fixation sites the time constants were much lower, reaching 17.4 ± 4 ms and 11.2 ± 3 ms for conditions F10 and F20, respectively (F10: N= 595, F20: N= 430). To

test for overall effects of fixation site and direction of deflection on decay time constant, we calculated a univariate, two-factorial analysis of variance (ANOVA). Fixation site was found to have a very strong effect ($F_{3,108} = 80.4$, $p < 0.001$), whereas the effect of deflection direction was weaker, though still statistically significant ($F_{3,108} = 4.7$, $p = 0.004$). The interaction between the two factors was not significant ($F_{7,216} = 1.6$, $p = 0.128$). Post-hoc Tamhane tests revealed no difference between conditions Pd and PF ($p = 0.789$), but highly significant differences between all other pairs of fixation-conditions ($p < 0.001$). Post-hoc Tamhane tests detected no significant difference between the deflection direction ($p > 0.593$).

3.5. Effect of haemolymph-pressure on damping

As the cross-sections in figure 3 illustrate, the antennal tissue is bathed in a volume of haemolymph. In order to test whether the biomechanics of the antenna might be affected by hydrostatic pressure of the haemolymph, we repeated the decay time course measurements in decapitated animals. Decapitation disconnected the head from thoracic and abdominal segments, in which the musculature of the body wall can alter hydrostatic pressure in the body cavity. Examples of decay time courses, recorded from the same decapitated animal, are shown on in figure 1 d. Decapitation had very little effect on antennal damping properties (see figure 4). Among the six animals tested, mean values of τ_{10} were 22.9 ± 5 ms and 25.3 ± 6 ms for conditions Pd and PF, respectively (Pd: N= 560; PF: N= 541). For distal fixation sites, the time constants were much lower, reaching 19.8 ± 6 ms and 12.4 ± 4 ms for fixations F10 and F20, respectively (F10: N= 542, F20: N= 420). Much like intact animals, fixation site was found to have a statistically significant effect on the time constant (ANOVA: $F_{3,88} = 54.1$, $p < 0.001$). Post-hoc testing revealed a weakly significant difference between conditions Pd and PF ($p = 0.042$). All other pairs of fixation sites differed significantly ($p < 0.001$, except for comparison of Pd and F10, where $p = 0.062$). In contrast to intact animals, direction of deflection had no effect (ANOVA: $F_{3,88} = 1.6$, $p = 0.195$). Direct comparison of median time constants in intact and decapitated animals revealed a weakly significant difference for the most distal fixation site F20 ($p = 0.026$) but not for the other three sites (Mann-Whitney-Test: Pd: $p = 0.099$; PF: $p = 0.646$, F10: $p = 0.054$; $N_1 = 7$, $N_2 = 6$).

3.6. Effect of desiccation on damping

Finally, we tried to remove the damping effect of the soft endocuticle by desiccation. We reasoned that

sufficient desiccation would remove all water from haemolymph and tissue, and most if not all water of the endocuticle, thus “tanning” the cuticle similar to the method previously described by Vincent and Wegst (2004).

Removal of haemolymph and tissue water decreased the flagellum weight by 47 % and the pedicel weight by 43 % (means). Removal of endocuticular water was expected to reduce damping (Vincent and Wegst, 2004). Figure 1 d shows that desiccation indeed caused a drastic reduction of damping. Dry flagella were always under-damped and exhibited oscillations. The resulting oscillatory curves were very similar within each insect.

In conditions Pd and PF, we identified two main frequency components in the Fourier spectrum (applying a standard FFT algorithm in MatLab to a data sets of 1024 sample points). In the example shown in figure 1 e, there was a dominating large-amplitude oscillation at 292 Hz and a low-amplitude oscillation at 1167 Hz. Among six animals tested, the low-frequency component ranged from 200 to 300 Hz, and the high-frequency component ranged from 900 to 1200 Hz. In condition F10, however, only one major oscillation frequency was observed. This ranged between 400 and 450 Hz (447 Hz in the example shown in figure 1 e). In all conditions, power spectra also contained additional low-power frequencies in the range between 25 to 75 Hz (see supplemental figure 7). As these components contributed very little power and did not change with fixation, they were neglected in this study.

In conclusion, damping of the antennal cuticle is strongest where the endocuticle layer is thickest, suggesting a possible role of the endocuticle in damping. De-capitation did not change the overall effect of fixation site on time constant, and only affected damping at the most distal site. Therefore, the differences in damping can not be a result of active control of the haemolymph pressure by thoracic or abdominal musculature. Finally, desiccation caused a transition from an over-damped regime to an under-damped regime, showing that loss of water strongly affects damping. The fact that the high-frequency component seen in conditions Pd or PF vanished in condition F10 suggests that the flagellum can be described by two coupled pendulums, one located in the proximal third of the flagellum (zone I) and a second one distal to that.

4. Conclusion

In this study we analyzed biomechanical properties of the stick-insect antenna and identify correlates in its morphological structure. We show that the flagellum is

over-damped in a manner that allows fast, oscillation-free return into its original shape after deformation. We find that the gradual change in damping along the flagellum correlates with cuticular features. This leads us to suggest that the distinct cuticular layers of the flagellum combine structural stiffness with strong damping, features of a biomechanical adaptation to the requirements for control and sensory information processing in an active tactile system: a straight posture in the instant of a new contact event, combined with a maximum of flexibility.

4.1. Histology and general damping properties of the flagellum

Our histological study of the antenna focussed on the ratio of endo- and exocuticle. It showed that the flagellum, in the main, consists of a tapered cone of stiff exocuticle lined by an inner wedge of compliant endocuticle. This inner wedge is thick at the proximal base of the antenna and thin at its distal half.

Our results show that mechanically deflected antennae from live *C. morosus* passively return to their initial posture when released without overshooting. The likelihood of oscillations increases and time constant decreases from proximal to distal fixation sites. In conjunction with the findings on differing cuticle layering, the results indicate a major influence of the soft endocuticle on the damping properties of the antenna. Fixation of the flagellum at different locations revealed that the return time constant at the base of the antenna was significantly higher ($\tau_{10} > 25$ ms) than in the distal half ($\tau_{10} < 18$ ms). Although a direct comparison of damping along the flagellum is strictly speaking not accurate, unless one compensates for modified dynamics and morphology, our results demonstrate the biomechanical effect of a cone-like morphology. In the context of tactile sensing, both time constants are short compared to the cycle frequency of antennal movements which ranges between 1 and 2 cycles per second during searching behaviour (Dürr et al., 2001) and increases to 5-8 cycles per second during tactile sampling (Schütz and Dürr, in press).

4.2. Effect of haemolymph-pressure

The antennae of stick insects are living tissue, actively controlled and moved by muscles attached to the base of the antennae (Dürr et al., 2001). To ensure a continuous supply of nutrients and gas exchange, haemolymph is actively pumped into the antennal segments using unidirectional pulsating organs located within the caput (Pass, 1985, 2000). These organs

control the steady haemolymph flow into the flagellum. Moreover, the gross haemolymph pressure within the body cavity is likely to be affected by contractions of the body wall musculature of the thorax and abdomen. If active control of haemolymph flow or haemolymph pressure within the body cavity contributed to the mechanical properties of the antenna, decapitation of the insect should have a significant effect on the measured time constants.

Our results showed that only the reflexion movements recorded after fixation at site F20 were significantly slower in decapitated than in intact animals. Hence there appears to be a small effect of haemolymph pressure on the distal flagellum, but the overall biomechanics of the antenna is not subject to active control of haemolymph pressure.

However, many pumping organs in insects are controlled autonomously (Pass, 2000). Observations of decapitated insects showed that, even after several hours, light mechanical stimuli could sometimes still induce active antennal movements, thus indicating the possibility of partly functional pumping organs. Thus, it is possible that complete inactivation of potential, autonomously generated haemolymph flow would have resulted in stronger differences between intact and decapitated animals. Further *in vivo* measurements of the haemolymph-pressure after decapitation are necessary to clarify this particular point.

4.3. Effect of desiccation

Insect cuticle is a natural composite material that covers a wide range of Young's moduli. Starting from very soft intersegmental membranes ($E \sim 1$ kPa, 40-75 % water content) up to the extremely stiff cuticle of the elytra ($E \sim 20$ GPa, 15-30 % water content), the physical properties of cuticle are morphologically adapted to the mechanical requirements of the structure (Vincent and Wegst, 2004). Several studies have shown that, besides restructuring of the cuticle components chitin and protein, desiccation can strongly affect the mechanical stiffness (Iconomidou et al., 2005; Jensen and Weisfogh, 1962; Vincent and Wegst, 2004; Vincent and Hillerton, 1979).

Here, desiccation of the antennae removed haemolymph and tissue water from both the exo- and the endocuticle, resulting in a structural change of the endocuticle's stiffness. Furthermore, it reduced the overall mass of the structure. After desiccation, the harmonic oscillating reflexion movements showed that the flagellum became under-damped. As even small changes in the water content of the untanned endocuticle can have a considerable effect on the

material properties (Jensen and Weisfogh, 1962), it is likely that the desiccation process strongly affected the elastic endocuticle with high its water content, making it more similar to the stiff exocuticle.

Reducing the water content of the elastic endocuticle layer changed the biomechanics of the antenna from a critically damped to an under-critically damped system. Our results show that the frequencies of these oscillations depend on the point of fixation, making the movements of the antenna very similar to those of a physical damped, harmonic oscillating leaf spring. This indicates that the mechanics of the flagellum can be abstracted with the model of a double pendulum with springs and dampers in both joints. Drying the cuticle increased the proportion of stiff cuticle within the proximal part of the antenna (0 to 10 mm from SP joint) thus increasing the resonance frequency of this part of the antenna. The distal part of the antenna (10 to 30 mm from the SP joint) was longer, consisting of less of the stiff cuticle and therefore showed a smaller resonance frequency.

The distinct differences between the movements of dried and un-dried antennae indicate a significant role of the strongly hydrated endocuticle in the damping of the antennae of *C. morosus*. Jensen and Weisfogh (1962) showed that reducing the water content of endocuticle by just 4 % had a noteworthy effect on the material properties. This is notably less than the observed weight loss of about 45 % in this study. However, further histological experiments need to quantify the exact water-loss and structural change of the flagellum's endocuticle.

Besides the material's properties, the geometric configuration of the antenna might also play an important biomechanical role. The cone-like morphology of the antenna itself might affect damping and stiffness of the whole structure. For lobsters it has been shown that their tapered antennal design helps to distinguish between bending of the flagellum due to contact and bending due to flow of the surrounding water (Barnes et al., 2001). Finite element analysis, combining the data of morphology, histology and mechanics could help to further clarify this point for insect antennae, too.

The results of this study indicate that a composite biological material consisting of stiff encasement and soft core, as found in the antennae of *C. morosus* plays an important role in determining the biomechanical properties of the structure. It allows a long, stiff structure to be easily displaced and bent when in contact, while insuring fast, non-oscillatory return to the original shape. Interestingly, long and thin plant stems seem to benefit from similar damping properties of composite-materials as do insect antennae (Bruchert et al., 2003; Spatz and Speck, 2002; Speck and Spatz, 2004). This

indicates that the principle of combining materials with distinct properties to merge the advantages of a stiff structure with advantageous damping properties might have evolved analogously in skeletal structures of animals and plants.

The results and conclusions of this study might help further understanding and modeling of the complex morphology of long and thin structures such as insect antennae, and at the same time inspire engineers to design and improve biological inspired technical active tactile sensors (Bonorno et al., 2008; Cowan et al., 2006; Fox et al., 2009; Kim and Möller, 2007; Lee et al., 2008; Okada and Toh, 2006; Solomon and Hartmann, 2006).

5. Acknowledgements

The authors would like to acknowledge Annelie Exter for her help in preparing the histological samples of the antennae. This study was financially supported by two bionics innovation projects, funded by the German Ministry of Research and Education (BMBF grants 0311969 and 0313766 to VD), a scholarship of the German National Academic Foundation and a postdoctoral fellowship of the "Irish Research Council for Science, Engineering and Technology" (both to JHD). We would also like to thank the anonymous reviewers for very constructive and helpful comments on the manuscript.

6. References

References

- Altner, H., Tichy, H., Altner, I., 1978. Lamellated outer dendritic segments of a sensory cell within a poreless thermo- and hygroreceptive sensillum of the insect *Carausius morosus*. *Cell & Tissue Research* 191, 287–304.
URL <http://dx.doi.org/10.1007/BF00222425>
- Barnes, T. G., Truong, T. Q., Adams, G. G., McGruer, N. E., 2001. Large deflection analysis of a biomimetic lobster robot antenna due to contact and flow. *Journal of Applied Mechanics-Transactions of the ASME* 68 (6), 948–951.
URL <http://dx.doi.org/10.1115/1.1406955>
- Bonorno, C., Brunetto, P., Fortuna, L., Giannone, P., Graziani, S., Strazzeri, S., JUL-AUG 2008. A tactile sensor for biomedical applications based on IPMCs. *IEEE Sensors Journal* 8 (7-8), 1486–1493.
URL <http://dx.doi.org/10.1109/JSEN.2008.920723>
- Bruchert, F., Speck, O., Spatz, H. C., 2003. Oscillations of plants' stems and their damping: theory and experimentation. *Philosophical Transactions of the Royal Society of London Series B-Biological Sciences* 358 (1437), 1487–1492.
URL <http://dx.doi.org/10.1098/rstb.2003.1348>
- Camhi, J. M., Johnson, E. N., 1999. High-frequency steering maneuvers mediated by tactile cues: Antennal wall-following by the cockroach. *Journal of Experimental Biology* 202 (5), 631–643.
- Cappe de Baillon, P., 1936. L'organe antennaire des Phasmes. *Bulletin biologique de la France et de la Belgique* 70, 1–35.
- Cowan, N., Lee, J., Full, R. J., 2006. Task-level control of rapid wall following in the american cockroach. *Journal of Experimental Biology* 209, 1617–1629.
URL <http://dx.doi.org/10.1242/jeb.02166>
- Dürr, V., König, Y., Kittmann, R., 2001. The antennal motor system of the stick insect *Carausius morosus*: anatomy and antennal movement pattern during walking. *Journal of Comparative Physiology A-Neuroethology Sensory Neural and Behavioral Physiology* 187 (2), 131–144.
URL <http://dx.doi.org/10.1007/s003590100183>
- Dürr, V., Krause, A. F., Neitzel, M., Lange, O., Reimann, B., 2007. Bionic tactile sensor for near-range search, localisation and material classification. In: Berns, K., Luksch, T. (Eds.), *Autonome Mobile Systeme 2007. Fachgespräch Kaiserslautern*, Springer, pp. 240–246.
URL http://dx.doi.org/10.1007/978-3-540-74764-2_37
- Dürr, V., Krause, A. F., Schmitz, J., Cruse, H., 2003. Neuroethological concepts and their transfer to walking machines. *International Journal of Robotics Research* 22 (3-4), 151–167.
URL <http://dx.doi.org/10.1177/0278364903022003002>
- Ferreira de Oliveira, J., Wajnberg, E., Motta de Souza Esquivel, D., Weinkauff, S., Winkhofer, M., Hanzlik, M., 2010. Ant antennae: are they sites for magnetoreception? *Journal of the Royal Society Interface* 7, 143–152.
URL <http://dx.doi.org/10.1098/rsif.2009.0102>
- Fox, C., Mitchinson, B., Pearson, M., Pipe, A., Prescott, T., 2009. Contact type dependency of texture classification in a whiskered mobile robot. *Autonomous Robots* 26, 223–239.
URL <http://dx.doi.org/10.1007/s10514-009-9109-z>
- Göpfert, M. C., Robert, D., 2001. Active auditory mechanics in mosquitoes. *Proceedings of the Royal Society of London B* 268, 333–339.
URL <http://dx.doi.org/10.1098/rspb.2000.1376>
- Hansson, B., 1999. *Insect Olfaction*. Springer, Berlin.
- Harley, C. M., English, B. A., Ritzmann, R. E., 2009. Characterization of obstacle negotiation behaviors in the cockroach, *Blaberus discoidalis*. *Journal of Experimental Biology* 212, 1463–1474.
URL <http://dx.doi.org/10.1242/jeb.028381>
- Heinzel, H. G., Gewecke, M., 1987. Aerodynamic and mechanical properties of the antennae as air-current sense-organs in *Locusta migratoria*. II. Dynamic characteristics. *Journal of Comparative Physiology A-Sensory Neural and Behavioral Physiology* 161 (5), 671–680.
URL <http://dx.doi.org/10.1007/BF00605008>
- Hellbach, S., Krause, A., Dürr, V., 2010. Feel like an insect: a bio-inspired tactile sensor system. In: *Proceedings of the International Conference on Neural Information Processing (ICONIP)*. Vol. 6444. Sydney, Australia, pp. 676–683.
URL http://dx.doi.org/10.1007/978-3-642-17534-3_83
- Hepburn, H. R., Chandler, H. D., 1976. Material properties of arthropod cuticles - arthroal membranes. *Journal of Comparative Physiology* 109 (2), 177–198.
URL <http://dx.doi.org/10.1007/BF00689417>
- Iconomidou, V. A., Willis, J. H., Hamodrakas, S. J., 2005. Unique features of the structural model of 'hard' cuticle proteins: implications for chitin-protein interactions and cross-linking in cuticle. *Insect Biochemistry and Molecular Biology* 35 (6), 553–560.
URL <http://dx.doi.org/10.1016/j.ibmb.2005.01.017>
- Imms, A. D., 1939. On the antennal musculature in insects and other arthropods. *Quarterly Journal of Microscopical Science* 81, 273–320.
- Jensen, M., Weisfogh, T., 1962. Biology and physics of Locust flight V: Strength and elasticity of locust cuticle. *Philosophical Transactions of the Royal Society of London Series B-Biological Sciences* 245 (721), 137–169.
URL <http://dx.doi.org/10.1098/rstb.1962.0008>
- Kim, D., Möller, R., 2007. Biomimetic whiskers for shape recognition. *Robotics and Autonomous Systems* 55 (3), 229–243.
URL <http://dx.doi.org/10.1016/j.robot.2006.08.001>
- Krause, A. F., Dürr, V., 2004. Tactile efficiency of insect antennae with two hinge joints. *Biological Cybernetics* 91 (3), 168–181.
URL <http://dx.doi.org/10.1007/s00422-004-0490-6>
- Lee, J., Sponberg, S. N., Loh, O. Y., Lamperski, A. G., Full, R. J., Cowan, N. J., 2008. Templates and anchors for antenna-based wall following in cockroaches and robots. *IEEE Transactions on Robotics and Automation Transactions on Robotics and Automation* 24 (1), 130–143.
URL <http://dx.doi.org/10.1109/TR0.2007.913981>
- Lin, H.-T., Dorfmann, A. L., Trimmer, B. A., Feb. 2009. Soft-cuticle biomechanics: A constitutive model of anisotropy for caterpillar integument. *Journal of Theoretical Biology* 256 (3), 447–457.
URL <http://dx.doi.org/10.1016/j.jtbi.2008.10.018>
- Loudon, C., 2005. Flexural stiffness of insect antennae. *American Entomologist* 51 (1), 48–49.
URL <http://www.entsoc.org/PDF/Pubs/Periodicals/AE/AE-2005/Spring/Loudon.pdf>
- Mayer, G., Sarikaya, M., 2002. Rigid biological composite materials: Structural examples for biomimetic design. *Experimental Mechanics* 42, 395–403.
URL <http://dx.doi.org/10.1007/BF02412144>
- Monteforti, G., Angeli, S., Petacchi, R., Minnocci, A., 2002. Ultrastructural characterization of antennal sensilla and immunocytochemical localization of a chemosensory protein in *Carausius morosus* Brunner (Phasmida : Phasmatidae). *Arthropod Structure & Development* 30 (3), 195–205.
URL [http://dx.doi.org/10.1016/S1467-8039\(01\)00036-6](http://dx.doi.org/10.1016/S1467-8039(01)00036-6)
- Mueller, M., Olek, M., Giersig, M., Schmitz, H., Aug. 2008.

- Micromechanical properties of consecutive layers in specialized insect cuticle: the gula of *Pachnoda marginata* (Coleoptera, Scarabaeidae) and the infrared sensilla of *Melanophila acuminata* (Coleoptera, Buprestidae). *Journal of Experimental Biology* 211 (16), 2576–2583.
URL <http://dx.doi.org/10.1242/jeb.020164>
- Mujagic, S., Krause, A. F., Dürr, V., 2007. Slanted joint axes of the stick insect antenna: an adaptation to tactile acuity. *Naturwissenschaften* 94 (4), 313–318.
URL <http://dx.doi.org/10.1007/s00114-006-0191-1>
- Okada, J., Toh, Y., 02 2006. Active tactile sensing for localization of objects by the cockroach antenna. *Journal of Comparative Physiology A*, 1–12.
URL <http://dx.doi.org/10.1007/s00359-006-0106-9>
- Pass, G., 1985. Gross and fine-structure of the antennal circulatory organ in cockroaches (Blattodea, Insecta). *Journal of Morphology* 185 (2), 255–268.
URL <http://dx.doi.org/10.1002/jmor.1051850210>
- Pass, G., 2000. Accessory pulsatile organs: Evolutionary innovations in insects. *Annual Review of Entomology* 45, 495–518.
URL <http://dx.doi.org/10.1146/annurev.ento.45.1.495>
- Pearson, M. J., Pipe, A. G., Melhuish, C., Mitchinson, B., Prescott, T. J., 2007. Whiskerbot: A robotic active touch system modeled on the rat whisker sensory system. *Adaptive Behaviour* 15 (3), 223–240.
URL <http://dx.doi.org/10.1177/1059712307082089>
- Pelletier, Y., Mcleod, C. D., 1994. Obstacle perception by insect antennae during terrestrial locomotion. *Physiological Entomology* 19 (4), 360–362.
URL <http://dx.doi.org/10.1111/j.1365-3032.1994.tb01063.x>
- Romeis, B., 1989. *Mikroskopische Technik*, 17th Edition. Urban & Schwarzenberg, München.
- Sandeman, D. C., 1976. Spatial equilibrium in the arthropods. In: Mill, P. J. (Ed.), *Structure and Function of Proprioceptors in the Invertebrates*. Chapman and Hall, London, pp. 485–527.
- Sandeman, D. C., 1989. Physical-properties, sensory receptors and tactile reflexes of the antenna of the Australian fresh-water crayfish *Cherax destructor*. *Journal of Experimental Biology* 141, 197–217.
- Schütz, C., Dürr, V., in press. Active tactile exploration for adaptive locomotion in the stick insect. *Proceedings of the Royal Society of London B*.
- Slifer, E. H., 1966. Sense organs on antennal flagellum of a walking-stick *Carausius morosus* Brunner Phasmida. *Journal of Morphology* 120 (2), 189–201.
URL <http://dx.doi.org/10.1002/jmor.1051200205>
- Solomon, J., Hartmann, M., 2006. Sensing features with robotic whiskers. *Nature* 443, 525.
URL <http://dx.doi.org/10.1038/443525a>
- Spatz, H. C., Speck, O., 2002. Oscillation frequencies of tapered plant stems. *American Journal of Botany* 89 (1), 1–11.
URL <http://dx.doi.org/10.3732/ajb.89.1.1>
- Speck, O., Spatz, H. C., 2004. Damped oscillations of the giant reed *Arundo donax* (Poaceae). *American Journal of Botany* 91 (6), 789–796.
URL <http://dx.doi.org/10.3732/ajb.91.6.789>
- Staudacher, E. M., Gebhardt, M., Dürr, V., 2005. Antennal movements and mechanoreception: Neurobiology of active tactile sensors. *Advances in Insect Physiology* 32, 49–205.
URL [http://dx.doi.org/10.1016/S0065-2806\(05\)32002-9](http://dx.doi.org/10.1016/S0065-2806(05)32002-9)
- Sun, J.-Y., Tong, J., Ma, Y., 2008. Nanomechanical behaviours of cuticle of three kinds of beetle. *Proceedings of the International Conference on Bionic Engineering*, 152–157.
URL [http://dx.doi.org/10.1016/S1672-6529\(08\)60087-6](http://dx.doi.org/10.1016/S1672-6529(08)60087-6)
- Tichy, H., 2007. Humidity-dependent cold cells on the antenna of the stick insect. *Journal of Neurophysiology* 97, 2851–3858.
URL <http://dx.doi.org/10.1152/jn.00097.2007>
- Vincent, J. F., Wegst, U. G., 2004. Design and mechanical properties of insect cuticle. *Arthropod Structure & Development* 33 (3), 187–199, *arthropod Locomotion Systems: from Biological Materials and Systems to Robotics*.
URL <http://dx.doi.org/10.1016/j.asd.2004.05.006>
- Vincent, J. F. V., Hillerton, J., 1979. Tanning of insect cuticle - critical-review and a revised mechanism. *Journal of Insect Physiology* 25 (8), 653–658.
URL [http://dx.doi.org/10.1016/0022-1910\(79\)90115-X](http://dx.doi.org/10.1016/0022-1910(79)90115-X)
- Weber, H., 1968. *Lehrbuch der Entomologie*. Gustav Fischer Verlag, Stuttgart.
- Weide, W., 1960. Einige Bemerkungen über die antennalen Sensillen sowie über das Fühlerwachstum der Stabheuschrecke *Carausius (Dixippus) morosus* br. (Insecta: Phasmida). *Wissenschaftliche Zeitschrift der Universität Halle IX*, 247–250.
- Williams, C. M., Kramer, E. M., 01 2010. The advantages of a tapered whisker. *PLoS ONE* 5 (1), e8806.
URL <http://dx.doi.org/10.1371/journal.pone.0008806>
- Zeil, J., Sandeman, R., Sandeman, D., 1985. Tactile localization - the function of active antennal movements in the crayfish *Cherax destructor*. *Journal of Comparative Physiology A-Sensory Neural and Behavioral Physiology* 157 (5), 607–617.
URL <http://dx.doi.org/10.1007/BF01351355>

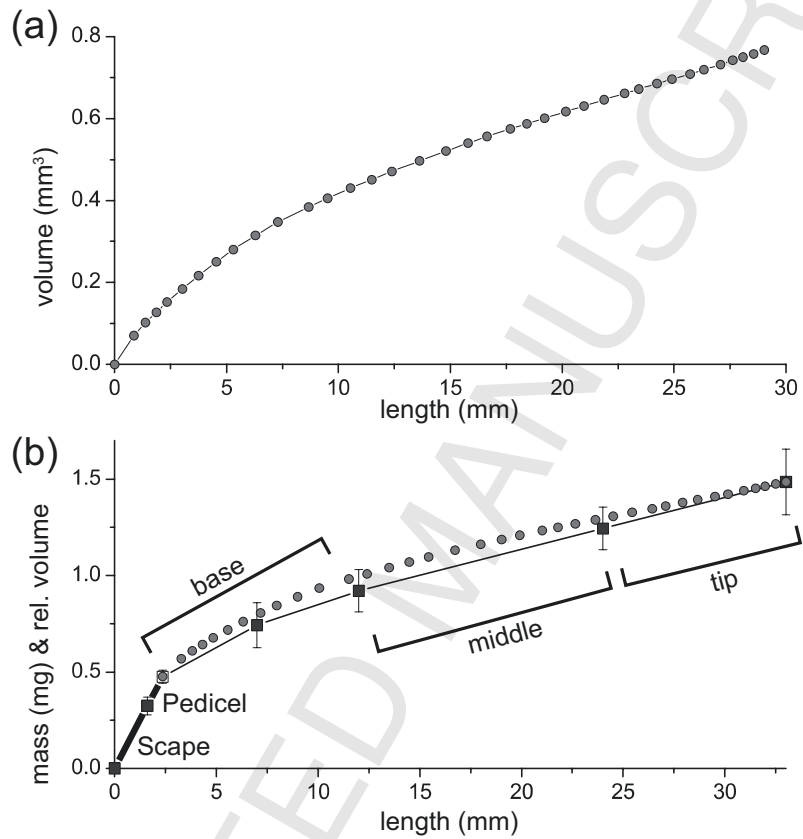


Figure 5: (supplemental figure) (a) The volume of the flagellum can be calculated from length and diameter values in figure 2, assuming a chain of cylinders, where the diameter of each cylinder is equivalent to the mid diameter of an annulus. (b) Mass of the antenna (squares), weighed in cumulative manner, and relative volume (circles), scaled to fit the length and mass ranges. The mass distribution along the flagellum is not even. As the increase of the mass differs from the increase of the volumes, the tapered shape of the flagellum alone cannot explain the change in mass. Rather, the fraction of mass attributed to cuticular and tissue structures increases.

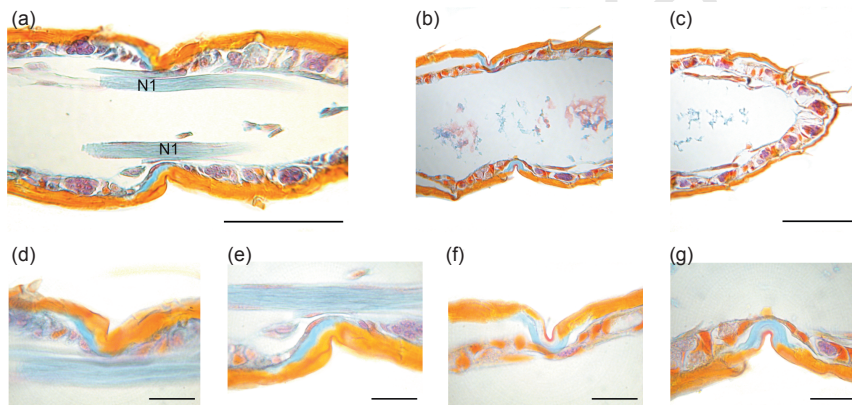


Figure 6: (supplemental figure) Representative longitudinal sections through medial and distal annulus junctions in the flagellum of *C. morosus*. Azan-stained paraffin sections of 10 μm thickness allow easy distinction of orange-coloured exocuticle and blue-coloured endocuticle. (a) middle flagellum region. (b) distal flagellum region. (c) tip region. Detail pictures of the lower row show annulus junctions of the middle flagellum region (d, e, zoomed in from a) and the distal flagellum region (f, g, zoomed in from b). Note that the junctions between adjacent annuli have thick exocuticle in the middle region of the flagellum. Only for distal annuli, the junctions are formed by a narrow joint-like membrane of endocuticle. N1: branches of the main antennal nerve. Scale bars are 100 μm (a to c) and 25 μm (d to g).

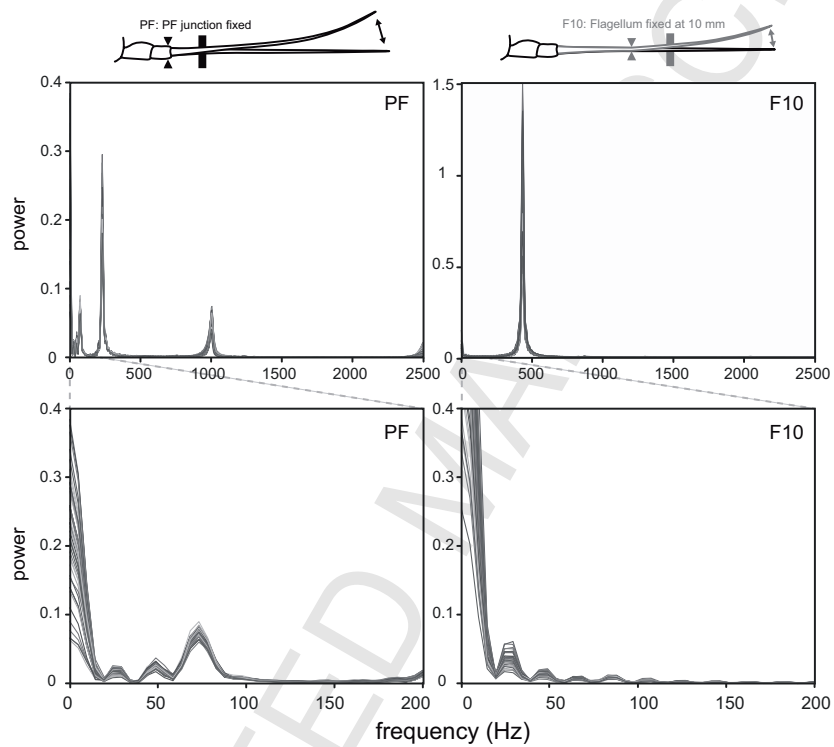


Figure 7: (supplemental figure) FFT-power-spectra of the oscillations of desiccated antennae, for fixation sites PF (left) and F10 (right). With the PF-joint fixed, the oscillations of dry antennae contain two major frequency components (292 and 1167 Hz). When fixed 10 mm more distally, oscillations were dominated by a frequency component of about 447 Hz. Note that the spectra of all measurements of a single preparation are superimposed, illustrating the very stereotypical mechanical behavior. The lower figures show magnifications of the frequency bands below 200 Hz.

Highlights:

The antenna consists of stiff exocuticle with an inner wedge of soft endocuticle.

Damping is stronger at the base of the antenna.

After experimental desiccation, the antenna becomes under-damped.

The antenna's cuticle properties are structural correlates of damping.

The biomechanical properties allow for straight posture and a maximum of flexibility.